PHYSICAL REVIEW B **94**, 235143 (2016)

Collapse of the Gd^{3+} ESR fine structure throughout the coherent temperature of the Gd-doped Kondo Semiconductor $CeFe_4P_{12}$

P. A. Venegas,[1,*] F. A. Garcia,[2] D. J. Garcia,[3] G. G. Cabrera,[4] M. A. Avila,[5] and C. Rettori[4,5]

[1]*UNESP-Universidade Estadual Paulista, Departamento de Física, Faculdade de Ciências, C.P. 473, 17033-360 Bauru, SP, Brazil*

[2]*IFUSP, Univ. de São Paulo, 05508-090 São Paulo, SP, Brazil*

[3]*Centro Atómico Bariloche (CNEA) and Instituto Balseiro (U. N. Cuyo), CONICET, CP 8400 Bariloche, Río Negro, Argentina*

[4]*Instituto de Física "Gleb Wataghin," UNICAMP, 13083-859, Campinas, SP, Brazil*

[5]*CCNH, Universidade Federal do ABC (UFABC), 09210-580 Santo André, SP, Brazil*

(Received 20 June 2016; revised manuscript received 1 November 2016; published 19 December 2016)

Recent experiments on Gd^{3+} electron-spin resonance (ESR) in the filled skutterudite $Ce_{1-x}Gd_xFe_4P_{12}$($x \approx 0.001$), at temperatures where the host resistivity manifests a smooth *insulator-metal* crossover, provide evidence of the underlying Kondo physics associated with this system. At low temperatures (below $T \approx 160$ K), $Ce_{1-x}Gd_xFe_4P_{12}$ behaves as a Kondo insulator with a relatively large hybridization gap, and the Gd^{3+} ESR spectra display a fine structure with Lorentzian line shape, typical of insulating media. In this work, based on previous experiments performed by the same group, we argue that the electronic gap may be attributed to the large hybridization present in the coherent regime of a Kondo lattice. Moreover, mean-field calculations suggest that the electron-phonon interaction is fundamental at explaining such hybridization. The resulting electronic structure is strongly temperature dependent, and at $T^* \approx 160$ K the system undergoes an insulator-to-metal transition induced by the withdrawal of $4f$ electrons from the Fermi volume, the system becoming metallic and nonmagnetic. The Gd^{3+} ESR fine structure coalesces into a single Dysonian resonance, as in metals. Our simulations suggest that exchange narrowing via the usual Korringa mechanism is not enough to describe the thermal behavior of the Gd^{3+} ESR spectra in the entire temperature region (4.2–300 K). We propose that the temperature activated fluctuating valence of the Ce ions is the key ingredient that fully describes this unique temperature dependence of the Gd^{3+} ESR fine structure.

DOI: 10.1103/PhysRevB.94.235143

I. INTRODUCTION

Among the strongly correlated electron systems, several rare-earth compounds, known as hybridization gap semiconductors or Kondo insulators/semiconductors, have recently attracted great interest [1–11]. Kondo insulators belong to a class of strongly correlated materials that form a group of either nonmagnetic semiconductors with a *narrow gap* or semimetals with tiny gaps. At low T, the Kondo lattice develops coherence throughout the system, forming a renormalized Fermi liquid, where conduction and $4f$ electrons contribute to the counting for the volume of the Fermi surface. Different from heavy fermions systems, in Kondo insulators the heavy-electron band is completely filled and the chemical potential falls in the middle of the hybridization gap (half-filling condition [12]). This semiconducting state manifests when the pseudogap straddles the Fermi energy, and is subjected to many-body renormalizations, leading to a T-dependent reduction of its magnitude [1,3–11,13–17]. Among interesting compounds with properties being related to this model are Ce-based filled skutterudite compounds [18]. They have the chemical formula REM_4X_{12} and crystallize in the $LaFe_4P_{12}$ structure, with space group $Im\bar{3}$ and local point symmetry T_h for the rare-earth (RE) ions [19]. The RE cations are usually referred to as *guest* or *filler* ions, and reside within the voids of the $[M_4X_{12}]$ polyanion *host* framework, or *cage* structure. Based upon simple electron counting, one can conclude that the series of Ce-based filled skutterudites CeM_4X_{12} for which M = Fe, Ru, Os and X = P, As, Sb are systems presenting a half-filled band in the presence of a $4f$ electron.

The low-T transport properties of these materials are similar to conventional semiconductors, but in contrast to what is expected from simple thermal activation, the gap seems to disappear at a temperature T^*, which is low relative to the gap size, indicating strong collective behavior [20,21]. Concerning $CeFe_4P_{12}$, its semiconducting properties at low T were considered anomalous when compared to other isostructural members of this class of compounds, most of which are metallic and magnetic [22]. The resistivity varies over six orders of magnitude between 50 and 300 K, but the data can only be fitted to an activated conduction process over a limited temperature range. This fitting yields a pseudogap of about 1500 K in magnitude, roughly three times smaller than the value predicted by LDA calculations [23], but in agreement with other experiments [24]. The magnetic susceptibility is nearly T independent over the range $100\,\text{K} < T < 300\,\text{K}$, clearly indicating that the ground state is nonmagnetic.

Lattice parameter deviations indicate mixed-valence character for the $4f$ element in all cases, which has also led to the definition of intermediate-valence semiconductors [25]. Recent studies of Ce and Sm compounds in this class of materials led to a renewed interest in this old hybridization gap (pseudogap) problem [1,2] and also to exotic types of Kondo effects [26]. Photoemission spectroscopy on single crystals of $CeFe_4P_{12}$ [1,22] showed a strong mixed-valence behavior of Ce ions, with a three-peak structure for the $4f$ level, with the presence of $4f^0$, $4f^1$, and $4f^2$ configurations due to the strong hybridization with the band. They found a mean occupation $n_f = 0.86$ for the $4f$ level, which is near the trivalent case

*Corresponding author: venegas@fc.unesp.br

as the nominal valence (a value of 3.14). In addition, the anomaly observed in the lattice parameter [3,27] and results from band-structure calculations [23] are also compatible with an intermediate valence for the Ce ions.

A topic of growing interest in the field of the skutterudites is to understand the interplay between their lattice dynamics and physical properties. Local vibrations of RE cations presumably indicate strong electron-phonon coupling that should be taken into account in any realistic picture. In $Ce_{1-x}Yb_xFe_4P_{12}$, *rattling* behavior is believed to account for the 20% reduction of the hyperfine parameters for the two Yb^{3+} sites observed in the electron spin resonance (ESR) experiments [28]. As for $La_{1-x}Gd_xPt_4Ge_{12}$, it was suggested to explain the evolution of the ESR linewidth as a function of temperature [29]. In any case, the energy scale of these vibrations are close to the so-called Einstein temperature (θ_E), obtained through the independent rattler approximation. In the case of Ce-based skutterudites, this characteristic energy scale is about 100 K and, in the particular case of $CeFe_4P_{12}$, $\theta_E = 148$ K, as probed by EXAFS studies [30]. Surprisingly, this temperature scale is about the same as the temperature $T^* \approx 150$ K, which marks the loss of coherence of heavy-fermion behavior, obtained from resistance experiments [20].

In a previous work on the ESR of Gd^{3+} in $Ce_{1-x}Gd_xFe_4P_{12}$ [31], it was shown that the low-T Gd^{3+} ESR spectra, composed of seven resolved insulatorlike Lorentzian lines, present temperature-activated behavior that yields a striking coalescence of the resolved fine structure into a single Dysonian (metalliclike) resonance at $T^* \approx 150$–160 K. This behavior is certainly related to the insulator-to-metal crossover induced by the loss of coherence, and exhibits the sensitivity of ESR experiments to probe such a remarkable effect. In this paper, we present numerical simulations for the collapse of the crystal-field fine structure of the Gd^{3+} ESR spectra in $Ce_{1-x}Gd_xFe_4P_{12}$ ($x \approx 0.001$) in the temperature range of interest. Our simulation shows the subtle and concomitant interplay between the Ce $4f$ fluctuation-valence (FV) and exchange-narrowing (EN) effects. The loss of coherence of the Fermi-liquid state, yielding a smooth insulator-metal (IM) transition at $T^* \approx 160$ K, gives further support to the assignment of $CeFe_4P_{12}$ as a Kondo semiconductor with a relatively large and T-dependent *pseudogap* [1,30,32]. This T dependence originates from many-body correlation effects in a Kondo lattice. At low T, long-range coherence effects develop among f electrons, so that they participate in band properties and a gap opens due to the strong hybridization with the conduction band. At half filling, the valence band is completely filled if one counts f and conduction electrons together and the system is an insulator. When the temperature is increased, changes of the electronic structure are produced, with the progressive filling of the gap at a lower temperature than would be expected from the simple thermal activation picture in conventional semiconductors [21]. An insulator-to-metal transition is induced at a coherence temperature T^* much lower than the Kondo temperature, marking the drop out of f electrons from the Fermi volume, leaving behind conducting holes in the valence band and localized f electrons at the RE ions [33]. In this regime, f electrons are nearly decoupled from the conduction band and stay in localized states relatively away from the Fermi level, which is purely of conduction electrons nature, with a nonzero but small density of states at E_F. We illustrate the above scenario with a hypothetical density of states (DOS) for temperatures below and above T^*. The qualitative picture is displayed in Fig. 1, showing results obtained with a model that accounts for the IM transition induced by electron-phonon coupling in $CeFe_4P_{12}$. The model is introduced in the next section. It qualitatively explains the role of lattice dynamics in affecting the electronic properties through strong coupling, and then, based on that model, we re-examine experimental results [31] in the whole temperature range 4.2–300 K.

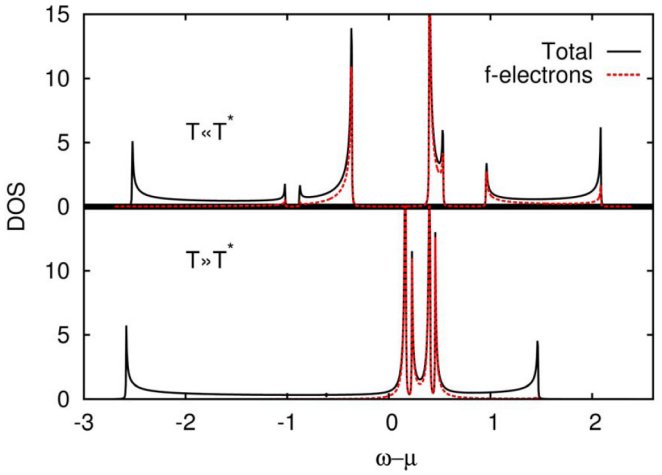

FIG. 1. Temperature-dependent properties of the DOS, showing in red the partial contribution of $4f$ electrons. For the low-T state ($T \leqslant T^*$), Ce $4f$ electrons participate in band properties. Hybridization effects are enhanced by the electron-phonon interaction, and a gap opens in the DOS (upper panel), the system becoming a Kondo insulator. The lower panel shows the high-T ($T \geqslant T^*$) behavior, where Ce $4f$-electron states decouple from the band and become localized, with a vanishingly small hybridization. The chemical potential μ moves inside the valence band, while the gap closes.

Lattice dynamics

The simplest model for the interplay between $4f$ orbitals and conduction electrons is the periodic Anderson model (PAM). The PAM [34,35] (also similar are the copper-oxide-like [36] and Kondo lattice models [37]) has been extensively studied. These studies show that antiferromagnetic or paramagnetic ground states are the probable states when the electronic concentration corresponds to half filling (one electron per orbital). Usually, to model PAM, one considers fully occupied rare-earth (RE) sites with $4f$ level below the Fermi level. However, spectroscopic experiments performed on those systems [1,22] suggest a $4f$ level above the Fermi level.

Electron-lattice coupling, the other essential ingredient, has been studied generically in the Su-Schrieffer-Heeger [38,39] model. In this model, lattice distortions are stable up to some critical temperature. The particular case of PAM, where lattice distortion couples to on-site energy and hopping, was discussed in Ref. [40], showing that the electron-lattice coupling suppresses the magnetic state. We find that the electron-lattice

coupling leads to a low-temperature paramagnetic insulator and a high-temperature metal at half filling. To illustrate the mechanism, we consider a simple one-dimensional geometry, although similar results can be obtained in more dimensions. To this end, we consider an array of RE $4f$ orbitals (corresponding to Ce^{3+} ions) coupled to a bath of conduction electrons. To qualitatively explain the experimental results, the inclusion of lattice distortions modifying the $4f$-conduction electrons hopping is crucial. The Hamiltonian considered reads

$$H = \sum_{\langle\langle i,l\rangle\rangle,\sigma} t_s c^\dagger_{i,\sigma} c_{l,\sigma} + \sum_{j,\sigma} E_f n_{d,j,\sigma} + \sum_{\langle\langle\langle i,l\rangle\rangle\rangle,\sigma} t_{sf} c^\dagger_{i,\sigma} d_{j,\sigma} + U \sum_j n_{d,\downarrow,j} n_{d,\uparrow,j} + \lambda \sum_j L_j . S_j + \sum_j 1/2 C {x_j}^2 + \text{H.c.},$$

where c operators refer to conduction electrons and d to $4f$-site orbitals. The first sum runs over the lattice sites i and l of the conduction electrons. The third sum runs over the lattice sites i of the conduction electrons and nearest neighbors j on RE of the so-defined zigzag chain. E_f is the RE on-site energy, t_s is the hopping between conduction electrons sites, and U is the on-site Coulomb repulsion for RE sites. λ is the coupling between the electronic spin $\mathbf{S}$ and the orbital angular moment $\mathbf{L}$ on the RE. The distortion x modifies the conduction electrons-RE hopping as $t_{sf} = t_{sf,0} - C g_2 x$. Assuming a uniform distortion and minimizing with respect to x results in $t_{sf} = t_{sf,0} - g_2^2(\langle c^\dagger d + d^\dagger c\rangle)$. Within this approximation, the temperature dependencies of x and t_{sf} are entirely given by the electronic thermodynamics.

We solve the resulting electronic Hamiltonian using a mean-field approximation:

$$H = \sum_{\langle\langle i,j\rangle\rangle,\sigma} t_s c^\dagger_{i,\sigma} c_{j,\sigma} + \sum_{i,\sigma} E_f n_{d,i,\sigma} + \sum_{\langle\langle\langle i,j\rangle\rangle\rangle,\sigma} t_{sf} c^\dagger_{i,\sigma} d_{j,\sigma} + U \sum_i (n_{d,\downarrow,i}\langle n_{d,\uparrow,i}\rangle + n_{d,\uparrow,i}\langle n_{d,\downarrow,i}\rangle - \langle n_{d,\downarrow,i}\rangle\langle n_{d,\uparrow,i}\rangle) + \lambda \sum_i [\langle L_{z,i}\rangle \frac{1}{2}(n_{d,\uparrow,i} - n_d, \downarrow, i)] + \text{H.c.},$$

where we decouple the on-site Coulomb repulsion as

$$n_{d,\uparrow,i} n_{d,\downarrow,i} \sim (n_{d,\downarrow,i}\langle n_{d,\uparrow,i}\rangle + n_{d,\uparrow,i}\langle n_{d,\downarrow,i}\rangle - \langle n_{d,\downarrow,i}\rangle\langle n_{d,\uparrow,i}\rangle).$$

We simplify the spin-orbit coupling to $L \cdot S \sim \langle L_z\rangle S_z = \langle L_z\rangle \frac{1}{2}(n_{d,\uparrow,i} - n_{d,\downarrow,i})$. When the RE occupation is low, $\langle L_z\rangle$ should be proportionally small, so we assume $\langle L_z\rangle \propto L\langle n_{d,i}\rangle (n_{d,i} = n_{d,\uparrow,i} + n_{d,\downarrow,i})$, where the magnitude of L is 3 for a rare earth. To allow for a possible antiferromagnetic (AF) order we consider two different sites for conduction electrons and RE ions (a four-site basis). To this end, we associate alternating angular moments $\pm\langle L_z\rangle$ to the RE sites (staggered order). The inclusion of the spin-orbit coupling is not essential. The main result is reproduced if this term is excluded: The IM transition with the lattice coupling is independent of λ. Without this $L \cdot S$ coupling the AF ordering is lost for the small value of U consider here. Any small value of $L \cdot S$ induces an AF ground state as expected from exact diagonalization methods [34]. We take a global density of one electron per site (four electrons on the four-site basis). The simplified Hamiltonian decouples up and down electrons. Due to the proposed alternating angular moments, the Hamiltonian has an up/down symmetry between different f sites:

$$n_{d,\sigma,1} = n_{d,-\sigma,2} \quad \text{where} \quad \sigma = \uparrow \text{ or } \downarrow.$$

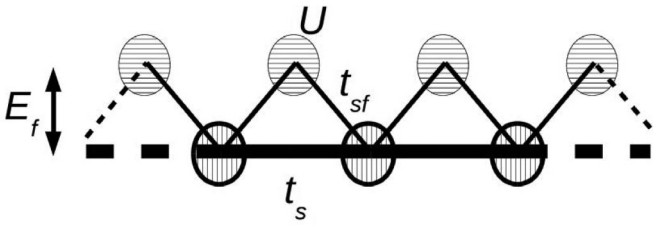

FIG. 2. Zigzag chain model. Circles indicate conduction electrons (bottom) and RE (top) sites. Parameters are shown in the figure.

To illustrate the physics of the IM transition in $CeFe_4P_{12}$ we use a zigzag chain (see Fig. 2).

The Hamiltonian can be readily diagonalized in Fourier space. The resulting k-space Hamiltonian is

$$H = \sum_{k,\sigma} [E_{f,\sigma,1} n_{d1,\sigma,k} + E_{f,\sigma,2} n_{d2,\sigma,k} + t_s(1 + e^{Ik}) c^\dagger_{1,\sigma,k} c_{2,\sigma,k} + t_{sf}(c^\dagger_{1,\sigma,k} d_{1,\sigma,k} + d^\dagger_{1,\sigma,k} c_{2,\sigma,k} + c^\dagger_{2\sigma,k} d_{2\sigma,k} + e^{Ik} d^\dagger_{2,\sigma,k} c_{1,\sigma,k}) + \text{H.c.}]$$

where $c_{1,\sigma,k}(d_{1,\sigma,k})$, $i = 1,2$, corresponds to the destruction operators for the two different conduction electrons (RE) sites of the basis. We take $t_s = 1$ as our energy unit. The parameters $t_{sf,0} = 0.05$ and $E_f = 0.5$ are chosen as to leave almost empty the $4f$ orbitals without any further interaction and to be compatible with a $4f$ state fluctuating between $4f^0$ and $4f^1$. The parameters $\frac{1}{2}\lambda L = 0.1$ and $U = 0.5$ are of order of magnitude of the size of the bandwidth as expected for RE ions [41].

We compare the cases of $g_2 = 0$ and $g_2 = 1$, for the uncoupled and the strongly coupled situations respectively, in order to assess the role of the electron-phonon coupling in the electronic structure. In this mean-field approximation, the on-site energies of the $4f$ orbitals are $E_{f,\sigma,1} = E_f + \frac{1}{2}\lambda L\langle n_{d1}\rangle + U\langle n_{d,-\sigma,1}\rangle$ and $E_{f,\sigma,2} = E_f - \frac{1}{2}\lambda L\langle n_{d2}\rangle + U\langle n_{d,-\sigma,2}\rangle$, and E_{f1} and E_{f2} must be determined self-consistently.

Figure 3 shows the low- and high-temperature dispersion relation with ($g_2 = 1$, dotted line) and without ($g_2 = 0$, full line) electron-lattice coupling. Flatter bands have mostly $4f$ character. The two flat bands split due to the spin-orbit coupling and the Coulomb repulsion. For $g_2 = 1$, bands have a mixed character with a large participation of $4f$ electrons (see also Fig. 1). This last state is known as the coherent regime in the Kondo and heavy fermion systems.

The electron-lattice coupling greatly enhances the hybridization and induces a gap between the valence and conduction bands at low T. With one particle per site, the

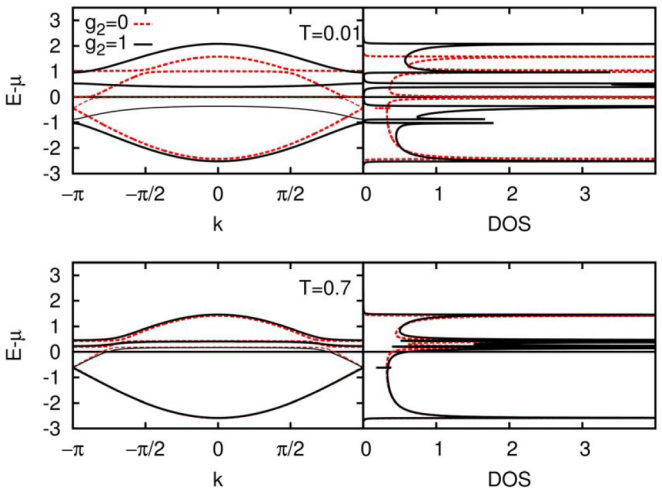

FIG. 3. Dispersion relation (left panels) and corresponding density of states (DOS $= \frac{-1}{\pi}\mathrm{Im}[G(\omega + 0.002I)]$, right panel). Full black (dashed red) lines correspond to the coupled (uncoupled) lattice and electron case. Top panels correspond to $T = 0.01$. Lower panels correspond to $T = 0.7$.

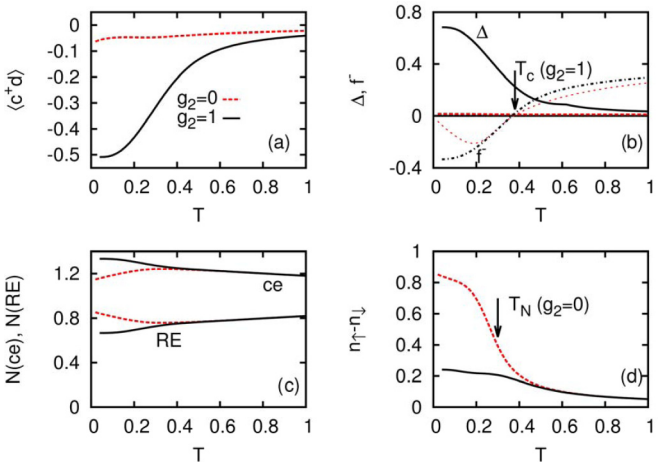

FIG. 4. Effect of temperature T on various properties of the model: (a) hybridization; (b) gap (continuous and dashed line) and highest energy of the second band (dotted and dash dotted line) with respect to the Fermi level. The second band is mainly of f character (see Fig. 3); (c) electron density in the conduction electron (upper curves) and RE (lower curves) sites; (d) polarization $(n_{d1,\uparrow} - n_{d1,\downarrow})$, black (red) line corresponds to the coupled (uncoupled) case. Hybridization in panel (a) and charge gap in panel (b) for the uncoupled case are very small (close to zero).

chemical potential falls between the second and third band (zero value in the energy axis). At this temperature the coupled system is an insulator. The gap between the second and third band is roughly proportional to t_{sf}^2. Without electron-lattice coupling the low-temperature gap is proportional to $t_{sf,0}$. The much larger gap in the coupled case is due to the fact that t_{sf} is dominated by $g_2^2(\langle c^\dagger d\rangle + \mathrm{H.c.})$, which in turn is much larger than $t_{sf,0}$.

At high temperature, both coupled and uncoupled dispersions are similar. This is due to a vanishing hybridization $\langle c^\dagger d\rangle$ with temperature [Fig. 4(a)], effectively decoupling electrons and lattice. The $g_2 = 1$ case becomes metallic as the highest state of the valence band [f^- in Fig. 6(b)] moves above the Fermi level [$T_c(g_2 = 1) \sim 0.4$]. The uncoupled case is always metallic, as the chemical potential falls inside the third band at low temperatures ($T < 0.4$) and inside the second band at higher temperatures.

The net charge on the conduction electrons and RE sites is similar in the coupled and uncoupled cases [Fig. 4(c)]. The RE charge is close to 0.8. With $g_2 = 0$, the RE magnetic moment is almost completely polarized on each site [Fig. 4(d)]. This magnetic moment decreases abruptly at high temperatures, signaling an AF transition [$T_N(g_2 = 0) \sim 0.3$]. When $g_2 = 1$, the RE polarization is strongly reduced. The temperature dependence of the RE polarization is weaker, with no appreciable variation at the IM transition temperature T_c. We identify the $g_2 = 1$ state with a paramagnetic state.

In the coupled case, the gap follows the hybridization trend. Both gap and hybridization decrease as the temperature increases. The hybridization goes to zero smoothly around $T \sim 0.4$ (coherence temperature) in the $g_2 = 1$ case, while in the uncoupled case the hybridization remains small. The gap between valence and conduction bands [Fig. 4(b)] is almost zero for the uncoupled case, while it has a strong temperature dependency for $g_2 = 1$. But note that it never closes completely.

A paramagnetic or AF ground state is expected from numerical results for the Anderson model [35] and Kondo lattice model [37]. Our results show that an Anderson-like model [34] (or more precisely copper-oxide-like [36]) coupled to lattice distortions describes an IM transition driven by the shift of the chemical potential. In agreement with Ref. [40], our results show that the AF order is suppressed with the electron-lattice coupling. As expected from [39,40], our solution shows a long-range distortion at low T. The large variation of the conduction electrons–RE hybridization with T, when $g_2 \neq 0$, is consistent with numerical results of Ref. [35].

No attempt has been made to use realistic values of parameters, since only a qualitative discussion is presented. Nevertheless, the present approach clarifies a key point, showing that the electron-lattice coupling is essential to the occurence of an IM transition in a paramagnetic state. The insulating state with a large charge gap at low T explains the almost temperature-independent linewidth of the ESR experiments in this temperature range. The IM transition marks the onset of a Korringa broadening at high temperatures, and the activated behavior of valence fluctuations of RE ions in the metallic regime is explained, since $4f$ states do not form a wide band, but instead are well localized above the Fermi level.

The IM transition reported in the literature [20,31] is qualitatively explained as the result of the coupling between the electronic hybridization and the lattice distortion. At the transition temperature, the gap between bands does not close. Instead, the onset of the metallic state is induced by the shift of the Fermi level to inner states of the valence band, due to the withdrawal of f electrons from the Fermi volume (loss of coherence). This explains the exponential fluctuations on the

rare-earth valence and global metallic behavior of $CeFe_4P_{12}$ above the IM transition as seen by ESR.

II. SIMULATION OF EXPERIMENTAL RESULTS AND ANALYSIS

The analysis of the ESR spectra of Gd^{3+} diluted in $CeFe_4P_{12}$ from 4.2 to 300 K requires consideration of three separate temperature regions to understand the T dependence of the observed spectra: (i) Below 150 K, the ESR spectra is consistent with Gd^{3+} ions diluted in insulators, i.e., there is no relaxation via conduction electrons (Korringa relaxation) [42,43]. The line shape associated to each fine structure of the spectrum is Lorentzian and the fully resolved spectra can be accounted for by the well-known anisotropic spin Hamiltonian for cubic symmetry [44]:

$$\mathcal{H} = \mu_B H g S + \tfrac{1}{60} b_4 \left(O_4^0 + 5O_4^4\right), \tag{1}$$

where the first term is the Zeeman energy, the second term is the fourth-order contribution of the cubic crystal field, with b_4 the fourth-order crystalline field parameter for Gd^{3+}, and O_4^0 and O_4^4 are the spin operators of fourth degree (note that for this specific cerium compound the sixth-order contribution of the cubic crystal field is canceled). (ii) Between ∼150 and ∼200 K, the observed fine structure coalesces into a single line of Dysonian shape, characteristic of ESR of diluted magnetic moments in metals [45,46]. (iii) above ∼200 K the single Dysonian line presents a nearly linear thermal broadening of the linewidth of ∼1 Oe/K, characteristic of a Korringa-like relaxation via conduction electrons.

Since the system is undergoing a "smooth" IM transition at about 150 K, the exchange interaction between Gd^{3+} local moments and conduction electrons must be considered. The Plefka-Barnes (PB) model, for the EN of the fine structure, is normally attempted to simulate such spectra [47–49]. Although we found that the PB model gives a good description of the thermal broadening of the linewidth for $T \geqslant 200$ K, it is not capable of reproducing the experimental details for the coalescence of the fine structure observed in the ESR spectra between 150 and 200 K [31]. Two discrepancies between the calculated and experimental spectra between 150 and 182 K can be noted: (i) using the PB theory the spectra still show a partially resolved fine structure where the experiment already displays a collapsed spectrum; (ii) the experiment shows a nonlinear thermal broadening of the spectra at the angle of collapsed fine structure [30° from the [001] direction in the (110) plane; see Fig. 5], whereas the PB theory shows a linear increase. Therefore, these results suggest that, besides the crystal-field and exchange coupling effects, one needs an additional and complementary mechanism in order to understand the coalescence of the Gd^{3+} ESR fine structure between ∼150 and ∼200 K.

The missing ingredient that can satisfactorily explain the experimental results is the fluctuating valence (FV) of the Ce ions in the filled skutterudite $CeFe_4P_{12}$. The mechanism leading to this FV is usually ascribed to the formation of the hybridization gap. However, in skutterudites, there is also the intriguing possibility that the coupling between the electronic state and the low-energy vibrations of the lattice may lead to FV and Kondo-like phenomena. In $CeFe_4P_{12}$, the picture

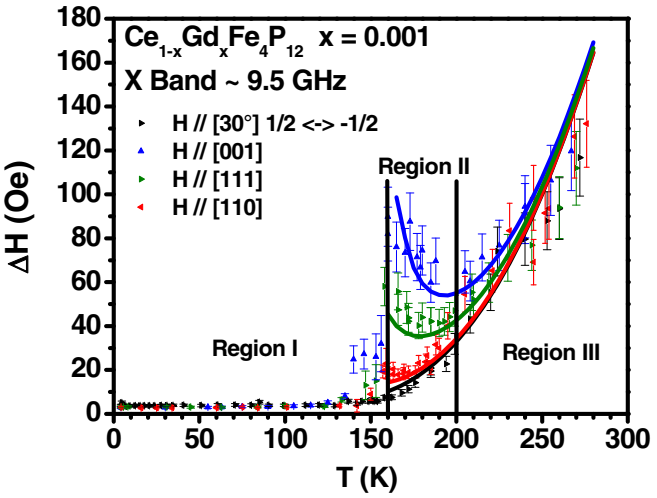

FIG. 5. ESR linewidth of $Ce_{1-x}Gd_xFe_4P_{12}$ ($x \approx 0.001$), triangles represents the experimental results [31]. Region I shows the ESR linewidth of transition $-\frac{1}{2} \leftrightarrow \frac{1}{2}$ for main crystal orientations. Full lines in regions II and III show theoretical simulations of the overall full linewidths of the collapsed spectra, including all ESR transitions.

obtained from spectroscopic experiments [1,22], indicates a large f-conduction electron hybridization strength. Below T^*, lattice vibrations cooperate coherently with the electronic insulating state, favoring the opening of the hybridization gap. Due to the large hybridization, Ce $4f$ electrons participate in band properties, hopping on and off between f states and the band, with strong fluctuations of the Ce valence. Despite one of the configurations being magnetic, it is known that these strong fluctuation effects quench the magnetic susceptibility [17,50], which remains practically constant with temperature, as observed in experiments [20]. This picture is also consistent with the unusual transport properties obtained in Ref. [32] for the thermoelectric power and the Hall carrier mobility, which are attributed to the $4f$-electron hybridization.

When $T \gg T^*$, our model indicates that f states decouple from the band and stay above the Fermi energy, the system being metallic (with a small density of states at μ) and nonmagnetic. *Rattling* of Ce ions is now incoherent and $4f$ states become localized. Since the hybridization is now small, the FV now implies an activation energy to move a band electron from the Fermi level to the f states (see Fig. 1). The simulation indicates that the above activation energy is weakly T dependent and can be approximated by its value at the insulator-to-metal transition (which we call E_{ex}).

Therefore, there are enough indicia to include in the simulation the effect of the FV of Ce ions on the Gd^{3+} ESR spectra. The formalism developed by Venegas *et al.* [51] can be considered as an additional T-dependent relaxation mechanism caused by the exchange interaction between the Gd^{3+} ion and the fluctuating Ce magnetic moments. This contribution to the Gd^{3+} ESR linewidth is approximated by an activation law, and is written as

$$\Delta H_{FV} = A e^{-E_{ex}/kT}, \tag{2}$$

where A is a constant and E_{ex} is the interconfigurational excitation energy discussed above.

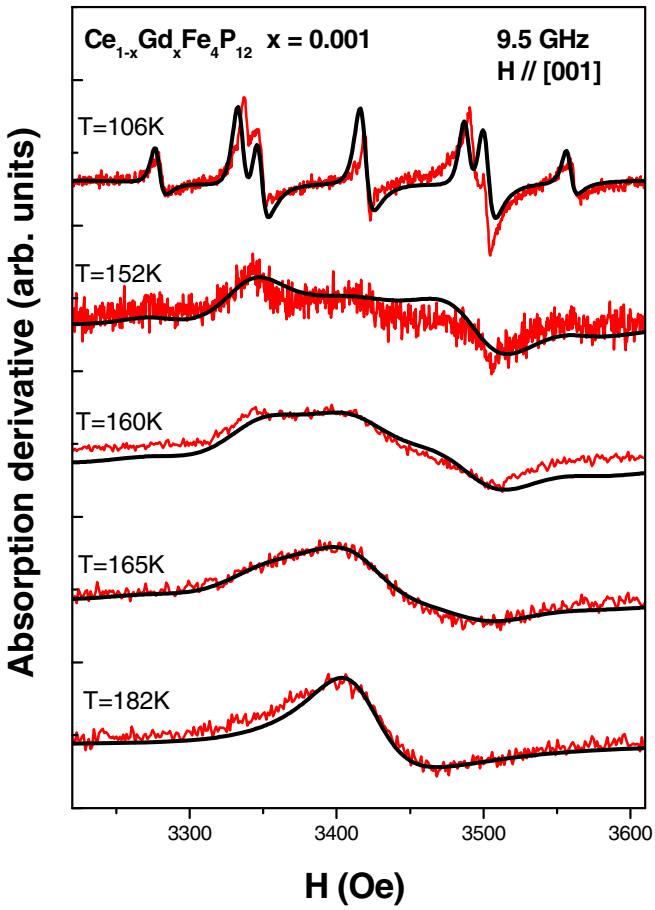

FIG. 6. ESR spectra of $Ce_{1-x}Gd_xFe_4P_{12}$ ($x \approx 0.001$) at different temperatures [31]. Full lines represent the theoretical model simulations.

Results for ΔH are shown in Fig. 5 for several orientations of the field. At low T, in the insulating regime, $T \leqslant T^*$ (region I), the linewidth of the $-\frac{1}{2} \leftrightarrow \frac{1}{2}$ transition is nearly constant, equal to a residual value, $\Delta H_{\rm res}$. At $T \approx T^*$, contributions including the Korringa rate, exchange narrowing (EN) effects, and activated FV mechanism begin to appear. The crystal-field effects on the Gd^{3+} fine structure are responsible for the angular dependence of ΔH, and at about $T \approx 200$ K, the line becomes nearly isotropic. An *apparent* Korringa behavior is displayed for $T \geqslant 200$ K, but our simulation suggests that the increase of the linewidth in region III should be ascribed to the activated FV exchange. The calculation of the overall ESR linewidth between ∼150 and ∼200 K, shown in Fig. 5, is much closer to the experimental data and considerably improved in comparison with the data analysis shown in Ref. [31].

The simulated spectra, within the same temperature range, are presented in Fig. 6. The agreement with experimental results from Ref. [31] is remarkable, including the collapse of the individual Gd^{3+} ESR fine-structure lines due to both EN and FV processes.

We have assumed that the conduction band starts becoming appreciably populated at $T^* = 160$ K. Therefore, the Korringa contribution to the linewidth starts at T^* and increases linearly with temperature, as $b(T - T^*)$. Following Urban *et al.* [31], narrowing effects are included in a phenomenological way, mimicking an effective Gd-Gd interaction, with a mean exchange field of 0.035 Oe and a mean width of ∼100 Oe, for the distribution of exchange fields. The overall linewidth is fitted to the expression

$$\Delta H = \Delta H_{\rm res} + b(T - T^*) + Ae^{-E_{\rm ex}/kT}, \qquad (3)$$

where $\Delta H_{\rm res}$ is the residual linewidth, b is the Korringa parameter, A is a constant, and $E_{\rm ex}$ is the interconfigurational excitation energy discussed above. The main parameters for optimal fitting obtained from simulations are listed in Table I.

TABLE I. Parameters obtained from the simulation of experimental results of the ESR spectra of Gd diluted in $CeFe_4P_{12}$. Values were extracted from calculations in the temperature range $4\,{\rm K} \leqslant T \leqslant 300$ K. The table includes parameters from Eqs. (1) and (3).

b (Oe/K)	$\Delta H_{\rm res}$ (Oe)	$E_{\rm ex}$ (K)	A (Oe)	b_4 (Oe)	g
0.05	5	1180	11 000	7	1.987

At this point we should mention that the fourth-order crystal-field parameter b_4 of Eq. (1) was kept constant and positive [52] throughout the simulations of the Gd^{3+} spectra in this Kondo semiconductor of relative large (insulatorlike) hybridization gap (∼1500 K). This positive value is in contrast to what is in general found for insulators and metals, where this parameter is usually found to be negative in insulators and positive in metals [53,54]. Hence, this is another anomalous example where the subtle and not well understood mechanism of crystal-field splitting of the Gd^{3+} excited states acts, via a $L \cdot S$ coupling, on the S-state ground state.

From Table I, the extracted Korringa rate is much smaller than the *apparent* Korringa rate of ∼1 Oe/K obtained for $T \gtrsim 200$ K. This is of key importance. The Korringa rate depends on $J_{fs}\eta_F$, the product of the f-conduction electron exchange interaction, and the density of states at the Fermi level. Then, the small extracted value implies either small J_{fs}, small η_F, or both. Therefore, the relatively large variation of ΔH for $T \gtrsim 200$ K is mainly associated with the influence of the FV mechanism of Ce ions on the Gd^{3+} ESR spectra. The extracted interconfigurational excitation energy of the Ce ions, $E_{\rm ex} = 1180$ K, illustrates the nature of the pseudogap as a full many-body concept. In the incoherent regime of the Kondo physics, f and conduction electrons states are mostly decoupled. While the Fermi surface is of conduction electrons nature, with a small density of states at the chemical potential μ, the excitation energy $E_{\rm ex}$ obtained in the simulation measures the distance from the Fermi level to the isolated f-electronic states. Remarkably, the ESR experiment captures both aspects of the same phenomenon: Korringa rate and EN effects due to conduction electrons, and FV exchange contributions [Eq. (2)] which come from the physics of the f-electronic structure.

III. CONCLUSIONS

Based on our previous ESR experiments in the $Ce_{1-x}Gd_xFe_4P_{12}$($x \approx 0.001$) skutterudite [31], we propose that the hybridization gap present in this Kondo semiconductor

is indeed strongly T dependent and closes with increasing temperatures. At $T = T^* \approx 160$ K, the gap is not completely closed, but the system undergoes an insulator-metal transition due to the dropout of f electrons from the Fermi volume, with the chemical potential shifting inward the valence band (see Fig. 1). This temperature T^* marks the loss of coherence, when f states decouple from the band and localize above the Fermi level. As a consequence, the system remains nonmagnetic due to the small weight of f states, which are practically empty in the ground configuration. Since the hybridization is small for $T \geqslant T^*$, the high-energy scale E_{ex} being probed by ESR experiments (of the order of 1000 K) is to be associated with the activated promotion of a conduction electrons from the Fermi level to the $4f^1$ magnetic configuration, leaving a hole in the conduction band. The presence of a temperature activated FV effect renders an extra exponential thermal broadening for the Gd^{3+} ESR linewidth. This allows us to simulate the coalescence of the Gd^{3+} fine structure in the ESR spectra and the change of the resonance line shape from Lorentzian (insulator media) to Dysonian (metallic media) at about the same temperatures where a smooth insulator-metal transition takes place. Just as importantly, by means of ESR measurements, we have obtained unequivocal experimental evidence for the presence of strong FV in a Kondo semiconductor, with the simultaneous identification of the coherence temperature T^* of the Kondo lattice. These results are further supported by a model that considers the coupling between localized states, itinerant electrons, and a lattice distortion.

ACKNOWLEDGMENT

The authors thank FAPESP (SP-Brazil), CNPq, and CAPES (Brazil), for financial support and NCC/GridUnesp (Brazil) for the computing resources.

[1] P. A. Rayjada, A. Chainani, M. Matsunami, M. Taguchi, S. Tsuda, T. Yokoya, S. Shin, H. Sugawara, and H. Sato, J. Phys.: Condens. Matter **22**, 095502 (2010).
[2] L. Degiorgi, Rev. Mod. Phys. **71**, 687 (1999).
[3] Z. Fisk, J. L. Sarrao, J. D. Thompson, D. Mandrus, M. F. Hundley, A. Miglori, B. Bucher, Z. Schlesinger, G. Aeppli, E. Bucher, J. F. DiTusa, C. S. Oglesby, H.-R. Ott, P. C. Canfield, and S. E. Brown, Phys. B (Amsterdam, Neth.) **206-207**, 798 (1995).
[4] G. Aeppli and Z. Fisk, Comments Condens. Matter Phys. **16**, 155 (1992).
[5] J. Robert, J.-M. Mignot, S. Petit, P. Steffens, T. Nishioka, R. Kobayashi, M. Matsumura, H. Tanida, D. Tanaka, and M. Sera, Phys. Rev. Lett. **109**, 267208 (2012).
[6] F. Strigari, T. Willers, Y. Muro, K. Yutani, T. Takabatake, Z. Hu, Y.-Y. Chin, S. Agrestini, H.-J. Lin, C. T. Chen, A. Tanaka, M. W. Haverkort, L. H. Tjeng, and A. Severing, Phys. Rev. B **86**, 081105 (2012).
[7] V. Guritanu, P. Wissgott, T. Weig, H. Winkler, J. Sichelschmidt, M. Scheffler, A. Prokofiev, S. Kimura, T. Iizuka, A. M. Strydom, M. Dressel, F. Steglich, K. Held, and S. Paschen, Phys. Rev. B **87**, 115129 (2013).
[8] H. Guo, H. Tanida, R. Kobayashi, I. Kawasaki, M. Sera, T. Nishioka, M. Matsumura, I. Watanabe, and Z. A. Xu, Phys. Rev. B **88**, 115206 (2013).
[9] J. Kawabata, T. Takabatake, K. Umeo, and Y. Muro, Phys. Rev. B **89**, 094404 (2014).
[10] A. Bhattacharyya, D. T. Adroja, A. M. Strydom, J. Kawabata, T. Takabatake, A. D. Hillier, V. Garcia Sakai, J. W. Taylor, and R. I. Smith, Phys. Rev. B **90**, 174422 (2014).
[11] H. Weng, J. Zhao, Z. Wang, Z. Fang, and X. Dai, Phys. Rev. Lett. **112**, 016403 (2014).
[12] P. Coleman, *Handbook of Magnetism and Advanced Magnetic Materials* (Wiley, New York, 2007).
[13] P. S. Riseborough, Phys. Rev. B **45**, 13984 (1992).
[14] P. S. Riseborough, Phys. B (Amsterdam, Neth.) **199-200**, 466 (1994).
[15] P. S. Riseborough, Phys. Rev. B **68**, 235213 (2003).
[16] M. F. Hundley, J. D. Thompson, P. C. Canfield, and Z. Fisk, Phys. B (Amsterdam, Neth.) **199-200**, 443 (1994).
[17] C. M. Varma, Rev. Mod. Phys. **48**, 219 (1976).
[18] H. Sugawara, S. Osaki, M. Kobayashi, T. Namiki, S. R. Saha, Y. Aoki, and H. Sato, Phys. Rev. B **71**, 125127 (2005).
[19] W. Jeitschko and D. Braun, Acta Crystallogr. B **33**, 3401 (1977).
[20] G. P. Meisner, M. S. Torikachvili, K. N. Yang, M. B. Maple, and R. P. Guertin, J. Appl. Phys. **57**, 3073 (1985).
[21] Z. Schlesinger, Z. Fisk, H.-T. Zhang, M. B. Maple, J. F. DiTusa, and G. Aeppli, Phys. Rev. Lett. **71**, 1748 (1993).
[22] M. Matsunami, K. Horiba, M. Taguchi, K. Yamamoto, A. Chainani, Y. Takata, Y. Senba, H. Ohashi, M. Yabashi, K. Tamasaku, Y. Nishino, D. Miwa, T. Ishikawa, E. Ikenaga, K. Kobayashi, H. Sugawara, H. Sato, H. Harima, and S. Shin, Phys. Rev. B **77**, 165126 (2008).
[23] L. Nordström and D. J. Singh, Phys. Rev. B **53**, 1103 (1996).
[24] S. V. Dordevic, N. R. Dilley, E. D. Bauer, D. N. Basov, M. B. Maple, and L. Degiorgi, Phys. Rev. B **60**, 11321 (1999).
[25] P. Wachter, *Handbook on the Physics and Chemistry of Rare Earths* (Elsevier, Amsterdam, 1994).
[26] D. L. Cox and A. Zawadowski, Adv. Phys. **47**, 599 (1998).
[27] F. Grandjean, A. Gérard, D. J. Braung, and W. Jeitschko, J. Phys. Chem. Solids **45**, 877 (1984).
[28] F. A. Garcia, D. J. Garcia, M. A. Avila, J. M. Vargas, P. G. Pagliuso, C. Rettori, M. C. G. Passeggi, S. B. Oseroff, P. Schlottmann, B. Alascio, and Z. Fisk, Phys. Rev. B **80**, 052401 (2009).
[29] F. A. Garcia, R. Gumeniuk, W. Schnelle, J. Sichelschmidt, A. Leithe-Jasper, Y. Grin, and F. Steglich, Phys. Rev. B **85**, 134402 (2012).
[30] D. Cao, F. Bridges, P. Chesler, S. Bushart, E. D. Bauer, and M. B. Maple, Phys. Rev. B **70**, 094109 (2004).
[31] F. A. Garcia, P. A. Venegas, P. G. Pagliuso, C. Rettori, Z. Fisk, P. Schlottmann, and S. B. Oseroff, Phys. Rev. B **84**, 125116 (2011).
[32] H. Sato, Y. Abe, H. Okada, T. D. Matsuda, K. Abe, H. Sugawara, and Y. Aoki, Phys. Rev. B **62**, 15125 (2000).
[33] C. Gröber and R. Eder, Phys. Rev. B **57**, R12659 (1998).
[34] M. Guerrero and R. M. Noack, Phys. Rev. B **53**, 3707 (1996).
[35] C. Huscroft, A. K. McMahan, and R. T. Scalettar, Phys. Rev. Lett. **82**, 2342 (1999).

[36] M. Guerrero and R. M. Noack, Phys. Rev. B **63**, 144423 (2001).
[37] H. Tsunetsugu, M. Sigrist, and K. Ueda, Rev. Mod. Phys. **69**, 809 (1997).
[38] W. P. Su, J. R. Schrieffer, and A. J. Heeger, Phys. Rev. B **22**, 2099 (1980).
[39] E. Fradkin and J. E. Hirsch, Phys. Rev. B **27**, 1680 (1983).
[40] P. Entel, H. J. Leder, and N. Grewe, Z. Phys. B: Condens. Matter **30**, 277 (1978).
[41] A. Abragam and B. Bleaney, *Electron Paramagnetic Resonance of Transition Ions* (Oxford University Press, Oxford, 1970).
[42] J. Korringa, Physica **16**, 601 (1950).
[43] H. Hasegawa, Prog. Theor. Phys. Kyoto **21**, 1093 (1959).
[44] P. Urban, D. Davidov, B. Elschner, T. Plefka, and G. Sperlich, Phys. Rev. B **12**, 72 (1975).
[45] R. H. Taylor, Adv. Phys. **24**, 681 (1975).
[46] S. E. Barnes, Adv. Phys. **30**, 801 (1981).
[47] T. Plefka, Phys. Status Solidi B **51**, K113 (1972).
[48] T. Plefka, Phys. Status Solidi B **55**, 129 (1973).
[49] S. E. Barnes, Phys. Rev. B **9**, 4789 (1974).
[50] M. B. Maple and D. Wohlleben, Phys. Rev. Lett. **27**, 511 (1971).
[51] P. A. Venegas and G. E. Barberis, Phys. Rev. B **46**, 911 (1992).
[52] R. N. de Mesquita, G. E. Barberis, C. Rettori, M. S. Torikachvili, and M. B. Maple, Solid State Commun. **74**, 1047 (1990).
[53] S. E. Barnes, K. Baberschke, and M. Hardiman, Phys. Rev. B **18**, 2409 (1978).
[54] G. E. Barberis, D. Davidov, C. Rettori, and J. F. Suassuna, Phys. Rev. B **19**, 2385 (1979).